Hydrodynamic (Wagner) impact of three-dimensional fluid and solid shapes.

Y.-M. Scolan[(1)], A.,A. Korobkin[(2)]
(1) ENSTA IPP IRDL (France), (2) UEA, (United Kingdom)
yves-marie.scolan@ensta.fr, A.Korobkin@uea.ac.uk

Highlights

- Hydrodynamic impact of 3D fluid/solid shapes,
- Analytical solutions of the Linearized Wagner problem,
- Approximation of shapes with elliptic paraboloids,
- Impact of breaking wave on a vertical circular cylinder.

1) Introduction

There are many situations where hydrodynamic impact cannot be simplified to a two-dimensional configuration. Even though the problem becomes simpler when one of the surfaces (fluid or solid) is flat, we may tackle more complex cases when both the fluid and solid surfaces are fully three-dimensional. As examples, we can consider a cylindrical plunging breaker hitting a monopile-type offshore wind turbine. Another case arises when a wave (not necessarily breaking) hits the superstructure (often circular cylinders) that link the columns of a floating wind turbine.
In these two cases the fluid/solid shapes can be approximated with two elliptic paraboloids about the initial contact point. Sometimes one or both of the elliptic paraboloids can degenerate into cylinders with a parabolic section, which is an aproximation of a circular cylinder. This is the purpose here to show that when two elliptic paraboloids hit at their respective summit, the solution of the linearized Wagner is still available analytically. Hence local and global loads can be calculated.
We consider the collision of two three-dimensional shapes in the frame of the Wagner approach (see Wagner, 1932). The application of the linearised Wagner problem is extended to 3D shapes, both of which can be approximated by an elliptic paraboloid equation at their initial point of contact. This configuration is illustrated below on the left side

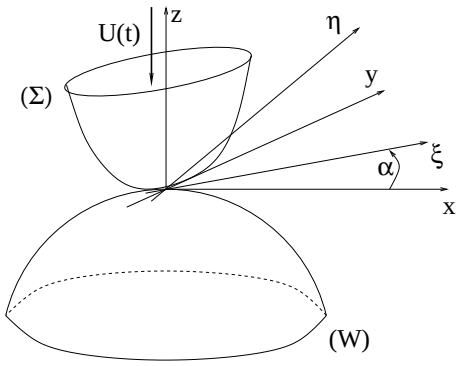

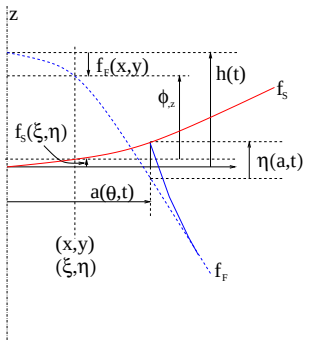

This problem has been investigated by Hertz (1881) for studying the impact of elastic bodies; it is known as the Hertz problem (see Goldsmith, Chap. 4). In the latter reference, the different configurations are described depending on the possible values of the curvature radii of the two colliding shapes. Indeed as the curvature radii can vary from zero to infinity a wide range of configurations can be covered.
In the present abstract, we formulate the linearized Wagner problem and exhibit the analytical solutions when both shapes are elliptic paraboloids.

2) Method of solution

The general equation of an elliptic paraboloid is $z = px^2 + qxy + ry^2$ where (p, q, r) determine the curvature radii at the origin $(x, y) = (0, 0)$ and the orientation of the 2 symmetry axes in the plane (x, y). Since we want to make sure to avoid a saddle point at the origin, we set $q = 0$ and then the orientation is defined separately. The solid elliptic paraboloid denoted Σ is defined by the equation

$$z = f_S(\xi, \eta) = \frac{\xi^2}{2r_x} + \frac{\eta^2}{2r_y}, \qquad r_x > 0,\ r_y > 0, \tag{1}$$

We denote α the angle of the axis ξ with respect to the axis x. With complex notation the rotation follows from $(x + iy) = e^{i\alpha}(\xi + i\eta)$.
We consider the relative vertical motion of the two shapes. For sake of simplicity, the solid shape is moving downwards whereas the fluid shape is at rest. The vertical velocity is denoted $U(t)$ and the corresponding relative motion is $h(t) = \int_0^t U(\tau)d\tau$. There is contact at $x = y = 0$ and $\xi = \eta = 0$ when $z = 0$ for both shape. That sets also the initial instant $t = 0$ at which the fluid-structure interaction starts. The equation of the fluid shape is

$$z = f_F(x, y) = -\frac{x^2}{2R_x} - \frac{y^2}{2R_y}, \qquad R_x > 0,\ R_y > 0, \tag{2}$$

The kinematic condition on the linearized expanding wetted and impermeable surface is written for the displacement potential ϕ. As illustrated in the right figure above, this is a Neumann condition formulated at a position (x, y) and its corresponding rotated position (ξ, η) ; it reads

$$\phi_{,z} = -h(t) + f_S(\xi, \eta) - f_F(x, y) \tag{3}$$

We choose here the horizontal coordinate system (x, y) to express the right hand side of (3). In order to remove the cross product xy, we rotate the coordinate system with angle β according to the relation $(X + iY) = e^{i\beta}(x + iy)$. By using the notations below, the angular rotation β follows from the formula

$$\frac{1}{r} = \frac{1}{r_y} - \frac{1}{r_x}, \quad \frac{1}{R} = \frac{1}{R_y} - \frac{1}{R_x}, \quad \gamma = \frac{r}{R}, \quad \tan 2\beta = -\frac{\sin 2\alpha}{\gamma + \cos 2\alpha} \tag{4}$$

The next figure shows the surface obtained by plotting the function $\beta = F(\gamma, \alpha)$.

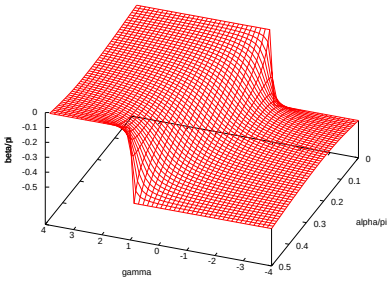

It is clear that $|\gamma| \leq 1$, is the critical range of the problem, however β is continuous with the parameters (α, γ) in the domain $\gamma \in \mathbb{R}$ and $\alpha \in]0, \pi/2[$. The two values $\alpha = 0$ and $\alpha = \pi/2$ are the two limiting cases since they correspond to the collinearity of the symmetry axes ; therefore no rotation is required. Actually the interval of variation of α can reduce to $[0, \pi/4]$.
We now pose the BVP in a coordinate system (X, Y) rotated with angle β from the initial (x, y) coordinate system. In that coordinate system the part of the RHS in (3) that represents the shape function is denoted

$$AX^2 + BY^2, \quad \text{with} \quad \left\{ \begin{array}{rcl} A + B & = & \frac{1}{2R_x} + \frac{1}{2R_y} + \frac{1}{2r_x} + \frac{1}{2r_y} \\ A - B & = & -\frac{1}{2r}\sqrt{\gamma^2 + 2\gamma\cos 2\alpha + 1} \end{array} \right. \tag{5}$$

Obviously for the present applications A and B are both positive. Some attention must be paid on the sign of $A-B$ which can be also calculated from $A-B=\frac{1}{2r}\frac{\sin 2\alpha}{\sin 2\beta}$. From the figure above it is shown that α and β are opposite in sign, hence $A-B$ and r are also opposite in sign. In Scolan (2014) the case $\gamma=1$ is studied when an elliptic paraboloid hits the crest of a cylindrical wave.

The method of solution of the BVP is quite standard since it is known from Korobkin (2002) that the wetted surface is elliptical as soon as the Neumann condition (3) can be written in the canonical form $\phi_{,z}=-H(t)+AX^2+BY^2$. Here the positive parameters A and B depend on the current geometry and H contains not only the penetration depth but possibly all quantities that depend only on time. In that case, the shape of the elliptic paraboloid described in the (X,Y) coordinate system, evolves over time as well, and the method of solution remains unchanged as shown in Scolan and Korobkin (2015). Indeed there is no reason not to consider that the two bodies (solid and fluid) can move along their six degrees of freedom as long as the initial contact point is at their highest/lowest point. The same method of solution can be duplicated here. However the all 16 quantities (namely (r_x, r_y, R_x, R_y) and the 6 DoF for each body, fluid and solid) do not vary over time independently since the expression (5), must keep the same form.

3) Illustrative results

We consider an overturning crest (leading to a plunging breaker) that hits a vertical circular cylinder. The free surface motion is generated in a closed tank from a dambreaking flow with a code described in Scolan *et al* (2007). This simulated flow is two dimensional and the left vertical wall of the closed tank partly accounts for the presence of the vertical cylinder. In particular this left wall allows to simulate the run-up along the cylinder. For the same initial condition but tuning the length of the tank, we can end up with a large variety of configurations. Actually we can cover all the configurations identified in Moalemi *et al* (2024). Here we keep only those for which the impact model developed above can apply. This is illustrated in the left figure below that shows the last computed free surface profile for several tank lengths.

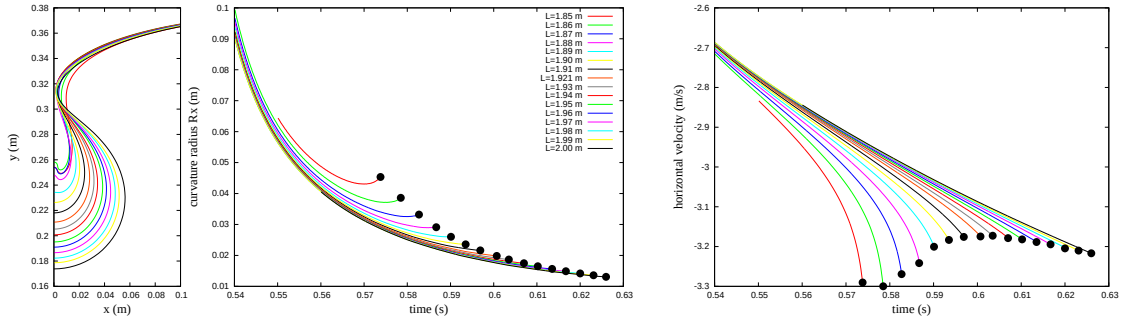

It should be noted that flip-through phenomenon occurs even though a pocket has formed. The middle and right figures above show the time variation of the curvature radius and horizontal velocity at the crest for each simulation before the last stages described in the left figure ; the wall significantly influences the fluid kinematics and the shape of the impacting wave. The maximum final velocity is obtained when Omega like free surface profile has formed. The force can be computed for a constant cylinder radius $r_y=0.05m$ that is larger than the greatest curvature radius of the wave crest, hence $r_y>R_x$ always. The ratio $|\gamma|=\frac{R_x}{r_y}$ corresponds to the parameter k_γ^2 defined in Scolan and Korobkin (2001) ; it is linked to the aspect ratio $k=a/b$ of the elliptic wetted surface and (a,b) are given as follows

$$a=\sqrt{2R_xh\left(1+k^2\frac{\mathrm{D}(e)}{\mathrm{E}(e)}\right)},\quad b=\sqrt{2r_yh\left(2-k^2\frac{\mathrm{D}(e)}{\mathrm{E}(e)}\right)},\quad e^2=1-k^2, \tag{6}$$

where the functions E and D of the eccentricity e, are the standard Elliptic integral as defined in Gradshteyn and Ryzhik (1994). From these variables, we can determine the added mass and force acting along the z axis

$$F(t) = -\frac{d}{dt}\left(M_a \dot{h}\right), \quad M_a(t) = \frac{2\pi}{3}\frac{\rho a^2 b}{E(e)}, \tag{7}$$

We "freeze" the configuration at the last computed free surface profile, the radius of curvature is set to a constant value R_x and the velocity $U = \dot{h}$ is constant as well. The corresponding values are those of the black dot in the figures above. As a consequence, the size of the elliptic wetted surface (a, b) and force F vary over time as $\sqrt{t}$; say $a(t) = a_o\sqrt{t}$ for the small semi-length and $F(t) = F_o\sqrt{t}$. It is worth reminding that the linearized Wagner model is valid during the early stage of the fluid-structure interaction, as long as $h(t) = Ut$ is small compared to the length scale of the wetted surface; this is true when $\sqrt{t} \ll a_o/U$.

For the above data, we compute the variation of the force factor F_o in terms of k_γ^2 . The figures below show the variation of the lengths of the wetted surface (a_o, b_o) (left) and the force F_o (right) for the different k_γ^2.

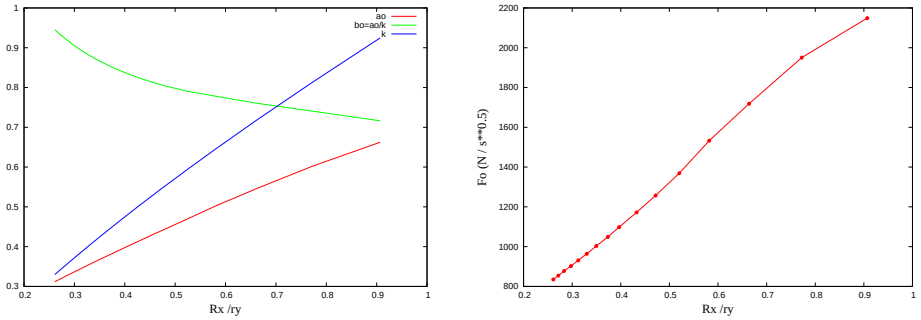

It is well known that the leading order expression (7) overestimates the force. Alternatively, a better estimate of the force follows from the integration of the pressure over the wetted surface. MLM or composite formulations of the pressure can then be used. This will be done in future works.

4) References

• Wagner, H. 1932 Über Stoss- und Gleitvorgänge an der Oberfläche von Flüssigkeiten. *ZAMM* **12**, pp. 193-215.

• Hertz H., 1881, Über die Berührung Fester Elastischer Körper, Journal für die reine und angewandte Mathematik, Vol. 92, pp 156-171.

• Goldsmith W., 1961. Impact : The Theory and Physical Behaviour of Colliding Solids. Arnold, London. 1960. 379 pp.

• Scolan Y.-M. & Korobkin A.A., 2001, Three-dimensional theory of water impact. Part 1. Inverse Wagner problem. J. Fluid Mech, 440, pp 293-326. https ://doi.org/10.1017/S002211200100475X

• Scolan Y.-M. and Korobkin A. A., Water entry of a body which moves in more than six degrees of freedom, **471**, Proc. R. Soc. A, http ://doi.org/10.1098/rspa.2015.0058

• Korobkin, A.A., 2002, "The entry of an elliptic paraboloid into a liquid at variable velocity", J. Appl. Math. and Mech., Vol.66, No. 1, pp. 39-48.

• Gradshteyn, I.S. & Ryzhik, I.M. 1994 *Tables of integrals* 5^{th} edition, Academic Press, 1204pp.

• Scolan Y.-M., 2014, Hydrodynamic impact of an elliptic paraboloid on cylindrical waves. J. Fluids Structures, 48, DOI : 10.1016/j.jfluidstructs.2014.04.007.

• Scolan Y.-M., O. Kimmoun, H. Branger, F. Remy, 2007, Nonlinear free surface motions close to a vertical wall. 22^{nd} International Workshop on Water Waves and Floating Bodies, Plitvice, Croatia, 15 April – 18 April 2007

• Moalemi A, Bredmose H, Kristiansen T, Pierella F. Wave front perturbation effect on the variability of monopile wave impact loads. J. Fluid Mech, 2024 ;984 :A65. doi :10.1017/jfm.2024.113